

## Molecular Dynamics Simulation Studies of Zeolite A. VII. Structure and Dynamics of H<sup>+</sup> ions in a Non-Rigid Dehydrated H<sub>12</sub>-A Zeolite Framework

Song Hi Lee\* and Sang Gu Choi†

*Department of Chemistry, Kyungsoong University, Pusan 608-736, Korea*

*†Department of Industrial Safety, Yangsan Junior College, Yangsan 626-800, Korea*

*Received October 23, 1998*

In the present paper, we report a molecular dynamics (MD) simulation study for the structure and dynamics of H<sup>+</sup> ions in non-rigid dehydrated H<sub>12</sub>-A zeolite framework at 298.15 K, using the same method we used in our previous studies of rigid and non-rigid zeolite-A frameworks. It is found that two different structures appear, depending on the choice of the Lennard-Jones parameter ( $\sigma$ ) for the H<sup>+</sup> ion, as is also observed in the study of rigid dehydrated H<sub>12</sub>-A zeolite framework, but the ranges of  $\sigma$  are different for the two structures. It is also found that some of the H<sup>+</sup> ions exchanged their sites without changing the number of H<sup>+</sup> ions at each site. The agreement between experimental and calculated structural parameters for non-rigid dehydrated H<sub>12</sub>-A zeolite is generally quite good. The calculated IR spectrum by Fourier transform of the total dipole moment auto-correlation function shows two major peaks, one around 2700 cm<sup>-1</sup> and the other around 7000 cm<sup>-1</sup>. The former appears in the calculated IR spectra of non-rigid zeolite-A framework only system and the latter remains unexplained except, perhaps, as an indication of a new formation of a vibrational mode of the framework due to the adsorption of the H<sup>+</sup> ions.

### Introduction

In a previous paper,<sup>1</sup> we reported a molecular dynamics (MD) simulation study of non-rigid zeolite-A framework only as the base case for a consistent study of the role of intraframework interaction on several zeolite-A systems, using the same method we used in our previous studies of rigid zeolite-A frameworks.<sup>2-6</sup> Usual bond stretching, bond angle bending, torsional rotational, and non-bonded Lennard-Jones and electrostatic interactions were considered as intraframework interaction potentials. The reproduced positions of the zeolite-A framework atoms by our MD simulation were in good agreement with those of the experiment.<sup>7</sup> The radial distribution functions and mean square displacements of the non-rigid zeolite-A framework atoms were characterized by the vibrational motion of the framework atoms. The up-and-down motion of the framework atoms from the center of  $\alpha$ -cage and the back-and-forth motion on each ring window from the center of each window were well described by the displacement auto-correlation and neighbor-correlation functions. IR spectrum was calculated by Fourier transform of the total dipole moment auto-correlation function of zeolite-A framework from our MD simulation and it showed that the simple harmonic oscillation of the correlation function results in a large peak at 2700 cm<sup>-1</sup>, which reflects a monotonous dynamical feature of the framework.

The structure of H<sup>+</sup> ions in a rigid dehydrate zeolite-A framework was studied by our MD simulation method.<sup>6</sup> Two kinds of structures appeared, with each type determined the choice of the Lennard-Jones parameter,  $\sigma$ , for the H<sup>+</sup> ion. For the smaller values of  $\sigma$ , the 12th H<sup>+</sup> ion was located on one of the 8-ring window sites, which was already occupied

by another H<sup>+</sup> ion; for the larger values of  $\sigma$ , it was located at one of the opposite-4-ring sites with the remaining 11 H<sup>+</sup> ions almost fixed near their initial position.

The inclusion of the intraframework interaction of zeolite systems is essential in taking account of energy exchange between the adsorbed molecules and the framework atoms, dynamical couplings of the sorbate with framework vibrations, and the flexibility of the host lattice. In a previous study,<sup>8</sup> an accurate valence force field for zeolite was presented by Nicholas *et al.* The force field contained terms for bond stretching, bond angle bending, torsional rotational, and non-bonded Lennard-Jones and electrostatic interactions. They found that the force field accurately reproduced the structure and dynamics of silica sodalite by the comparison of experimental data with theoretical infrared (IR) spectra, radial distribution functions, and mean-square displacements.

Recently Faux *et al.*<sup>9</sup> reported MD simulations of fully hydrated and dehydrated Na<sup>+</sup>-zeolite 4A with a mobile zeolite framework at 298 K and a steepest descent energy minimization simulation on the dehydrated zeolite. They found that the optimized structure yielded bond lengths, bond angles, and positions of sodium ions, which were in very good agreement with the published X-ray data.<sup>3,10</sup> In fact, after our present work was begun, they published their report, but our work differs in the interaction potentials for the framework atoms.

In our MD simulation studies of zeolite-A systems with rigid zeolite-A frameworks<sup>2-6</sup> and with non-rigid zeolite-A framework only,<sup>1</sup> we present MD simulation of H<sub>12</sub>-A using non-rigid dehydrated zeolite-A framework. The primary purpose of this work is to provide the basic non-rigid zeolite-A framework, to test several intraframework interactions of H<sub>12</sub>-A zeolite framework, and to investigate the local struc-

ture and dynamics of H<sup>+</sup> ions in the non-rigid zeolite-A framework.

In Section II we present the molecular models and MD simulation method. We discuss our simulation results in Section III and present the concluding remarks in Section IV.

### Molecular Models and Molecular Dynamics Simulations

The structure of zeolite-A framework is modeled by the pseudo cell, (SiAlO<sub>4</sub>)<sub>12</sub>, using the space group Pm $\bar{3}$ m (a = 12.2775 Å). The Si and Al atoms are assumed to be identical (denoted as T) because the Ewald summation<sup>11</sup> is valid with this assumption. Since the zeolite-A framework is not assumed to be rigid, the framework atoms (T and O) are subject to move according to the equation of motion. The initial positions of the framework atoms and H<sup>+</sup> ions are those determined by the X-ray diffraction experiment of Pluth and Smith<sup>7</sup> for the dehydrated zeolite-A system are used.

The interaction potential for the framework atoms is given by the sum of bond stretching, bond angle bending, torsional rotational, and non-bonded Lennard-Jones (LJ) and electrostatic interactions. The usual LJ parameters and the electrostatic charges for the Coulomb potential are used in our previous studies<sup>1-6</sup> with the Ewald summation,<sup>11</sup> and they are given in Table 1. In the pseudo cell, (TO<sub>2</sub>)<sub>24</sub>, 24 T atoms, give a total of 96 T-O bonds. The T-O bond lengths of the TO<sub>4</sub> tetrahedra differ according to the O atoms: T-O(1) = 0.16591, T-O(2) = 0.16531, and T-O(3 or 3') = 0.16688 nm. The T-O bond stretching potential is given by a simple harmonic potential

$$V(r) = \frac{k_r}{2}(r_{T-O} - r_{eq})^2 \quad (1)$$

where  $k_r = 250,000$  kJ/mol·nm<sup>2</sup> and  $r_{eq}$  is used for each T-O bond length.

Since each TO<sub>4</sub> tetrahedron gives 6 O-T-O angles, a total of 144 O-T-O angles exists in the pseudo cell, (TO<sub>4</sub>)<sub>24</sub>. The O-T-O angles are O(1)-T-O(2) = 108.13, O(1)-T-O(3 or 3') = 111.70, O(2)-T-O(3 or 3') = 107.12, and O(3)-T-O(3') = 110.83 degrees. The O-T-O bond angle bending potential is also given by a simple harmonic potential<sup>8</sup>

$$V(\theta) = \frac{k_\theta}{2}(\theta - \theta_{eq})^2 \quad (2)$$

**Table 1.** Lennard-Jones parameters and electrostatic charges used in this study

| atom           | $\sigma$ (Å) | $\epsilon$ (kJ/mol) | charge (e) |
|----------------|--------------|---------------------|------------|
| H <sup>+</sup> | 0.6 and 1.4  | 0.0657              | 0.55       |
| Al(=Si)        | 4.009        | 0.5336              | 0.6081     |
| O(1)           | 2.890        | 0.6487              | -0.4431    |
| O(2)           | 2.890        | 0.6487              | -0.4473    |
| O(3)           | 2.890        | 0.6487              | -0.4380    |

where  $k_\theta = 0.17605$  kJ/mol·deg<sup>2</sup> and  $\theta_{eq}$  is used for each O-T-O bond angle.

Each O atom gives a T-O-T angle and a total of 48 T-O-T angles exists in the pseudo cell, (TO<sub>2</sub>)<sub>24</sub>. The T-O-T angles are T-O(1)-T = 142.08, T-O(2)-T = 164.18, and T-O(3 or 3')-T = 145.55 degrees. According to Nicholas et al.,<sup>8</sup> the T-O-T bond angle bending potential is given by an anharmonic potential

$$V(\theta) = \frac{k_{\theta 1}}{2}(\theta - \theta_{eq})^2 - \frac{k_{\theta 2}}{2}(\theta - \theta_{eq})^3 + \frac{k_{\theta 3}}{2}(\theta - \theta_{eq})^4 \quad (3)$$

where  $k_{\theta 1} = 0.013829$  kJ/mol·deg<sup>2</sup>,  $k_{\theta 2} = 0.00050542$  kJ/mol·deg<sup>3</sup>,  $k_{\theta 3} = 0.000005148$  kJ/mol·deg<sup>4</sup> and  $\theta_{eq}$  is used for each T-O-T bond angle.

In silicates, the Si-O bond is known to lengthen as the Si-O-Si bond angle becomes smaller.<sup>12</sup> The exact relationship between the bond length and bond angle depends on the compound and also varies with the amount of Al in the lattice. In order to reproduce the correct dynamic behavior of the lattice, it is found that the Urey-Bradley term is needed, based on the T-T non-bonded distance for each T-O-T angle

$$V(r) = \frac{k_r}{2}(r_{T-T} - r_{eq})^2 \quad (4)$$

where  $k_r = 22,845$  kJ/mol·nm<sup>2</sup> and  $r_{eq}$  is used for each T-T distance -0.31381, 0.32747, and 0.31878 nm.

In a dihedral angle, which is associated to four consecutive atoms (O-T<sup>\*</sup>-O<sup>\*</sup>-T), a torsional rotational potential on the T<sup>\*</sup>-O<sup>\*</sup> bond is possible since the three O atoms connected to T<sup>\*</sup>, except the O<sup>\*</sup> atom, are restricted by the O-T<sup>\*</sup>-O angle bending potentials. In the pseudo cell, (TO<sub>2</sub>)<sub>24</sub>, there are 48 T-O-T angles. Since we can pick up one among three O atoms connected to each T atom to make a dihedral angle, there can be a total of 96 dihedral angles. The torsional rotational potential for the O-T-O-T dihedral angle is a periodic function with a 3-fold barrier:

$$V(\phi) = \frac{k_\phi}{2}[1 - \cos(3\phi)] \quad (5)$$

where  $k_\phi = -2.9289$  kJ/mol. The corresponding forces due to the potentials of Eqs. (1)-(5) are obtained by differentiation with respect to the position vector of each site.<sup>13</sup>

A canonical ensemble of fixed N (number of particles), V (volume of fixed zeolite framework), and T (temperature) is chosen for the simulation ensemble. Gauss's principle of least constraint<sup>14</sup> is used to maintain the system at a constant temperature. The ordinary periodic boundary condition in the x-, y-, and z-direction and minimum image convention are applied for the Lennard-Jones potential with a spherical cut-off of radius equal to half of each simulation box length. Gear's fifth order predictor-corrector method<sup>15</sup> is used to solve the equations of translational motion of the framework atoms with a time step of 2.00×10<sup>-16</sup> second. The equilibrium properties are averaged over five blocks of 100,000 time steps, for a total of 500,000 time steps after 500,000 time steps to reach an equilibrium state. The configuration of each ion is stored every 5 time steps for further analyses.

## Results and Discussion

The preliminary molecular dynamics (MD) simulations for several values for the Lennard-Jones parameter,  $\sigma$ , for the  $H^+$  ion varying from 0.6 Å to 1.8 Å were carried out in order to examine the structural change of the  $H^+$  ions in the non-rigid dehydrated zeolite-A framework. As a result, two distinctly different structures in the arrangement of the 12  $H^+$  ions were found: for the larger values of  $\sigma$  (1.3-1.8 Å), the 12th  $H^+$  ion is at one of the opposite-4-ring sites, which indicates that all the  $H^+$  ions are near their initial positions during the MD simulations, and, on the other hand, for the smaller values of  $\sigma$  (1.0-1.2 Å), the 12th  $H^+$  ion moves from one of the opposite-4-ring sites to one of the 8-ring window sites, which is already occupied by one of 3  $H^+$  ions (the 9th, 10th, and 11th) with the remaining 11  $H^+$  ions kept near their initial positions.

It is worth noting, however, that as the value of  $\sigma$  decreased, some  $H^+$  ions exchanged their sites without changing the number of  $H^+$  ions at each site. In the case of  $\sigma = 1.0$  Å which is in the smaller  $\sigma$  value category, there are two  $H^+$  ions located at one of the three 8-ring window sites - one is the 11th  $H^+$  ion, which was initially located at the 8-ring window site, and the other is the 12th  $H^+$  ion, which came from one of the opposite-4-ring sites. Upon decreasing the value of  $\sigma$  to 0.6 Å, the 12th  $H^+$  ion moved from the 8-ring window site to one (+, -, - : occupied by the 8th  $H^+$  ion) of the 6-ring window sites, then the 8th  $H^+$  ion moved to another site (+, -, - : occupied by the 5th  $H^+$  ion) of the 6-ring window sites through the  $\beta$ -cage, and finally the 5th  $H^+$  ion moved to the 8-ring window site (see Figure 1). In a sense, this behavior of the  $H^+$  ions is similar to the "concerted transport process" at 600.0 K<sup>16</sup> in which upon increasing the temperature,  $Na_{III}$  type ion, initially bound to site III (opposite-4-ring), moved to one of the three neighboring 8-rings, and at the same time the  $Na_{II}$  type ion, initially bound to site II (8-ring), moved to another neighboring site III, with all the  $Na_I$  type ions remaining near their starting positions (6-ring).

In the case of rigid dehydrated  $H_{12}$ -A zeolite,<sup>6</sup> when the value of  $\sigma$  was reduced to 0.2 Å, a peculiar arrangement of 12  $H^+$  ions was observed - two  $H^+$  ions occupy one of the 6-ring window sites, one inward the  $\alpha$ -cage and the other outward the 6-ring window. Two  $H^+$  ions on the same 6-ring window site are not observed, probably due to the non-rigid-

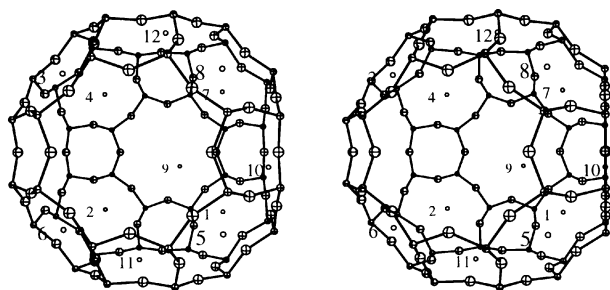


**Figure 1.** Stereoplot of 12  $H^+$  ions in the  $\alpha$ -cage of dehydrated  $H_{12}$ -A zeolite framework at 298.15 K.

ity of dehydrated zeolite-A framework. For example, neither the 12th and the 8th  $H^+$  ions nor the 8th and the 5th  $H^+$  ions are occupied on the same 6-ring window due to the continuous back-and-forth and up-and-down motions of the zeolite-A framework atoms as observed in the non-rigid zeolite-A framework only system.<sup>1</sup>

The main reason for the structural differences according to the values of  $\sigma$  is the repulsion between  $H^+$  ions, which determines the possibility of co-occupancy of two  $H^+$  ions on the same site. For example, in the case of rigid dehydrated  $H_{12}$ -A zeolite,<sup>6</sup> two  $H^+$  ions are not on the same site for  $\sigma = 0.8$ -2.0 Å, but are on the same 8-ring window site for  $\sigma = 0.4$ -0.7 Å and on the same 6-ring window site for  $\sigma = 0.2$  Å. The size of the 6-ring window site is relatively smaller than the size of the 8-ring window site. The second reason is the non-rigidity of the zeolite-A framework as discussed above.

We classified the 12  $H^+$  ions according to their locations as  $H_I$  for the 6-ring window sites,  $H_{II}$  for the 8-ring window sites, and  $H_{III}$  for the opposite-4-ring sites. Hence, for the larger values of  $\sigma$  (1.3-1.8 Å), there are 8  $H_I$  type ions, 3  $H_{II}$  type ions, and an  $H_{III}$  type ion, but for the smaller values of  $\sigma$  (0.6-1.2 Å), 8  $H_I$  type ions and 4  $H_{II}$  type ions without an  $H_{III}$  type ion. This result is very similar to that of rigid dehydrated  $H_{12}$ -A zeolite except the ranges of  $\sigma$ : the larger values of  $\sigma$  (0.8-2.0 Å) and the smaller values of  $\sigma$  (0.4-0.7 Å). We have selected two values of  $\sigma$  for the  $H^+$  ion, 0.6 Å and 1.4 Å, for our analysis of the energetic, structural, and dynamics properties of  $H^+$  ions in the non-rigid dehydrated  $H_{12}$ -A zeolite system.

Several potential energies are averaged for 500,000 time steps (100 ps) and are compared with those for the non-rigid zeolite-A framework only system<sup>1</sup> in Table 2. The adsorption of  $H^+$  ions into the non-rigid zeolite-A framework has affected mostly T-O bond stretching and T-O-T bond angle bending energies. The structural difference of the  $H^+$  ions for  $\sigma = 0.6$  Å and 1.4 Å appears primarily in O-T-O bond angle bending, in T-O bond stretching, and in  $H^+$ -frame Coulomb energies.

In Table 3, the results of the experimental<sup>7</sup> and calculated structural parameters of non-rigid dehydrated zeolite A are compared. The mean crystallographic positions and the mean-square displacement matrices  $\mathbf{B}$  are obtained by referring the values of the individual atoms back to the asymmetric unit by symmetry operations.<sup>17</sup> The elements of the symmetric  $3 \times 3$  matrix  $\mathbf{B}$  are computed as  $u_{ij} = \langle u_i u_j \rangle - \langle u_i \rangle \langle u_j \rangle$ . The agreement between the experimental and calculated coordinates for the zeolite-A framework atoms is generally quite good, but for the adsorbed cations the agreement is somewhat poor because of the difference between  $H^+$  and  $Na^+$  ions. In the comparison of the calculated coordinates for  $H^+$  ions between the rigid and non-rigid dehydrated zeolite-A frameworks, the results for  $H^+$  ions in the rigid dehydrated zeolite A are somewhat closer to those for  $H^+$  ions than in the non-rigid dehydrated zeolite A. The same trend is seen in calculated bond lengths of the rigid and non-rigid dehydrated zeolite-A frameworks in Table 4. The

**Table 2.** Average potential energies for 500,000 time steps (100 ps)

| interaction potential                        | potential energy (kJ/mol)  |                            |                             |
|--|----------------------------|----------------------------|-----------------------------|
|  | $\sigma = 0.6 \text{ \AA}$ | $\sigma = 1.4 \text{ \AA}$ | framework only <sup>a</sup> |
| H <sup>+</sup> -H <sup>+</sup> L.J potential | 0.0                        | 0.0                        | -                           |
| H <sup>+</sup> -H <sup>+</sup> Coulomb       | 327.3±0.2                  | 324.1±0.2                  | -                           |
| H <sup>+</sup> -frame L.J potential          | 44.5±0.2                   | 40.1±0.2                   | -                           |
| H <sup>+</sup> -frame Coulomb                | -1310.61±0.7               | -1126.6±1.7                | -                           |
| frame-frame L.J potential                    | -188.2±0.1                 | -187.9±0.1                 | -187.9±2.1                  |
| frame-frame Coulomb                          | 2358.1±0.2                 | 2353.9±0.4                 | 2502.1±4.8                  |
| T-O bond stretching                          | 236.1±5.5                  | 258.9±2.0                  | 133.3±8.2                   |
| T-T non-bonded stretching                    | 55.2±0.3                   | 52.6±0.2                   | 55.3±3.7                    |
| T-O-T bond angle bending                     | 22.7±0.1                   | 21.9±0.2                   | 37.3±2.2                    |
| O-T-O bond angle bending                     | 276.8±3.9                  | 186.0±0.5                  | 265.9±9.7                   |
| O-T-O-T torsional                            | -220.9±0.3                 | -216.6±0.2                 | -218.4±1.1                  |

<sup>a</sup>Reference [1]

anisotropy thermal parameters  $\beta_{ij}$  can be used to visualize the extent of the thermal motions and their anisotropy by the ORTEP computer code.<sup>18</sup>

In Table 4, we have compared experimental and calculated bond lengths of non-rigid dehydrated zeolite A. The calculated bond lengths are generally shorter than the experimental lengths except for H<sub>I</sub>-O(3) due to the difference of Na<sup>+</sup> and H<sup>+</sup>. The results for rigid dehydrated zeolite A is much better than those of the non-rigid.

Figure 2 shows mean square displacements (MSD) of H<sub>I</sub>, H<sub>II</sub>, and H<sub>III</sub> type ions in the non-rigid dehydrated zeolite-A framework atoms. The behavior of the MSD's is common: short, rapid increase and then very slow, flat movement, which indicates very small random motion in closed sites, but of different kinds. This is very similar to what has been found for Na<sup>+</sup> ions in rigid dehydrated zeolite A,<sup>2</sup> but the fluctuation after rapid increase is much smaller. MSD's of non-rigid dehydrated zeolite framework atoms (not shown) - T, O(1), O(2), and O(3) - show behavior very similar to that of H<sup>+</sup> ions with different magnitudes of MSD but much dif-

**Table 3.** Experimental and calculated structural parameters of non-rigid dehydrated zeolite A (a = 12.2775 Å)

| atom             | x/a                               | y/a    | z/a    | $\beta_{11}$ | $\beta_{22}$ | $\beta_{33}$ | $\beta_{12}$ | $\beta_{13}$ | $\beta_{23}$ |       |
|------------------|-----------------------------------|--------|--------|--------------|--------------|--------------|--------------|--------------|--------------|-------|
| T                | exp. <sup>a</sup>                 | 0      | 0.1836 | 0.3722       | 38           | 35           | 26           | 0            | 0            | 5     |
|                  | cal.( $\sigma=0.6 \text{ \AA}$ )  | 0.0134 | 0.1836 | 0.3731       | 24.9         | 23.0         | 5.5          | -4.4         | -4.4         | 19.8  |
|                  | cal.( $\sigma=1.4$ )              | 0.0134 | 0.1845 | 0.3737       | 35.2         | 23.4         | 4.1          | -3.7         | -4.1         | 35.3  |
|                  | cal. <sup>b</sup>                 | 0.0123 | 0.1792 | 0.3662       | 13.2         | 20.8         | 19.2         | -3.4         | -3.3         | 18.4  |
| O(1)             | exp. <sup>a</sup>                 | 0      | 0.2275 | 0.5          | 65           | 76           | 28           | 0            | 0            | 0     |
|                  | cal.( $\sigma=0.6$ )              | 0.0073 | 0.2303 | 0.4817       | 3.0          | 5.5          | -11.0        | 0.1          | -0.1         | -3.9  |
|                  | cal.( $\sigma=1.4$ )              | 0.0062 | 0.2325 | 0.4807       | 2.1          | 4.8          | -17.3        | 0.0          | 0.0          | -2.9  |
|                  | cal. <sup>b</sup>                 | 0.0044 | 0.2049 | 0.4829       | 1.1          | 2.4          | 1.4          | -0.5         | 0.0          | 0.1   |
| O(2)             | exp. <sup>a</sup>                 | 0      | 0.2910 | 0.2910       | 90           | 48           | 48           | 0            | 0            | 22    |
|                  | cal.( $\sigma=0.6$ )              | 0.0120 | 0.2885 | 0.2885       | 52.8         | 24.7         | 24.7         | 4.5          | 4.5          | 45.0  |
|                  | cal.( $\sigma=1.4$ )              | 0.0133 | 0.2872 | 0.2872       | 59.0         | 28.9         | 28.9         | 9.0          | 9.0          | 54.9  |
|                  | cal. <sup>b</sup>                 | 0.0108 | 0.2932 | 0.2879       | 66.9         | 46.8         | 52.1         | 16.5         | 17.5         | 48.7  |
| O(3)             | exp. <sup>a</sup>                 | 0.1119 | 0.1119 | 0.3437       | 52           | 52           | 56           | 11           | 3            | 3     |
|                  | cal.( $\sigma=0.6$ )              | 0.1116 | 0.1116 | 0.3459       | 27.2         | 27.2         | 61.6         | 38.7         | 17.6         | 17.6  |
|                  | cal.( $\sigma=1.4$ )              | 0.1116 | 0.1116 | 0.3912       | 24.1         | 24.1         | 63.0         | 39.0         | 14.6         | 14.6  |
|                  | cal. <sup>b</sup>                 | 0.1065 | 0.1065 | 0.3335       | 16.4         | 27.1         | 57.2         | 33.1         | 22.7         | 18.5  |
| H <sub>I</sub>   | exp. <sup>a</sup>                 | 0.1991 | 0.1991 | 0.1991       | 55           | 55           | 55           | 21           | 21           | 21    |
|                  | cal.( $\sigma=0.6$ )              | 0.2062 | 0.2062 | 0.2062       | 48.3         | 48.3         | 48.3         | 2.1          | 2.1          | 2.1   |
|                  | cal.( $\sigma=1.4$ )              | 0.2083 | 0.2083 | 0.2083       | 70.0         | 70.0         | 70.0         | -10.9        | -10.9        | -10.9 |
|                  | cal.( $\sigma=0.6$ ) <sup>c</sup> | 0.1991 | 0.1991 | 0.1991       |              |              |              |              |              |       |
|                  | cal.( $\sigma=1.1$ ) <sup>c</sup> | 0.2009 | 0.2009 | 0.2009       |              |              |              |              |              |       |
| H <sub>II</sub>  | exp. <sup>a</sup>                 | 0      | 0.4290 | 0.4290       | 238          | 177          | 177          | 0            | 0            | -64   |
|                  | cal.( $\sigma=0.6$ )              | 0.0193 | 0.3595 | 0.3595       | 129.6        | 42.2         | 42.2         | 3.5          | 3.5          | -23.4 |
|                  | cal.( $\sigma=1.4$ )              | 0.0207 | 0.3789 | 0.3789       | 140.7        | 31.9         | 31.9         | 4.4          | 4.4          | -12.8 |
|                  | cal.( $\sigma=0.6$ ) <sup>c</sup> | 0.0297 | 0.3404 | 0.3404       |              |              |              |              |              |       |
|                  | cal.( $\sigma=1.1$ ) <sup>c</sup> | 0.0175 | 0.4127 | 0.4127       |              |              |              |              |              |       |
| H <sub>III</sub> | exp. <sup>a</sup>                 | 0.5000 | 0.2087 | 0.2087       | 10           | 74           | 74           | 0            | 0            | -10   |
|                  | cal.( $\sigma=1.4$ )              | 0.4844 | 0.1546 | 0.1546       | 10.0         | 20.1         | 20.1         | 3.6          | 3.6          | -2.1  |
|                  | cal.( $\sigma=1.1$ ) <sup>c</sup> | 0.4967 | 0.1435 | 0.1435       |              |              |              |              |              |       |

<sup>a</sup> Experimental values for Na<sub>12</sub>-A zeolite [7]. <sup>b</sup> Non-rigid zeolite-A framework only [1]. <sup>c</sup> Rigid dehydrated H<sub>12</sub>-A zeolite [6]

**Table 4.** Experimental and calculated bond lengths ( $\text{\AA}$ ) of non-rigid dehydrated zeolite A

| bond length            | exp. <sup>a</sup> | non-rigid      |                | rigid <sup>b</sup> |                |
|------------------------|-------------------|----------------|----------------|--------------------|----------------|
|                        |                   | $\sigma = 0.6$ | $\sigma = 1.4$ | $\sigma = 0.6$     | $\sigma = 1.1$ |
| H <sub>I</sub> -O(3)   | 2.334(3)          | 2.375(266)     | 2.410(207)     | 2.333              | 2.337          |
| H <sub>I</sub> -O(2)   | 2.919(3)          | 2.780(237)     | 2.758(256)     | 2.919              | 2.921          |
| H <sub>II</sub> -O(2)  | 2.395(13)         | 1.236(209)     | 1.595(227)     | 0.932              | 2.124          |
| H <sub>II</sub> -O(1)  | 2.623(7)          | 2.185(238)     | 2.196(317)     | 2.428              | 2.523          |
| H <sub>III</sub> -O(3) | 2.551(34)         | -              | 1.857(223)     | -                  | 1.957          |
| H <sub>III</sub> -O(1) | 2.573(33)         | -              | 2.034(405)     | -                  | 2.042          |
| H <sub>I</sub> -H      | 3.698(4)          | -              | 3.598(318)     | -                  | 3.766          |

<sup>a</sup> Experimental values for Na<sub>12</sub>-A zeolite [7]. <sup>b</sup> Rigid dehydrated H<sub>12</sub>-A zeolite [6].

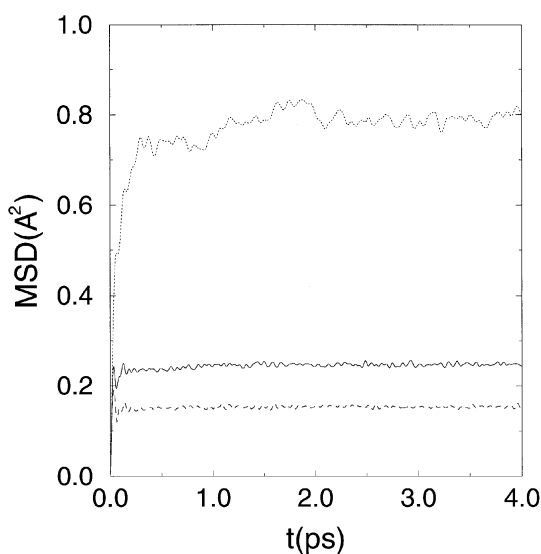


**Figure 2.** Mean square displacements (MSD) of three types of H<sup>+</sup> ions in non-rigid dehydrated, H<sub>12</sub>-A zeolite at 298.15 K. — : H<sub>I</sub>, ..... : H<sub>II</sub>, and - - - - : H<sub>III</sub>.

ferent from the behavior of non-rigid zeolite-A framework only system, which is all periodic.<sup>1</sup> This indicates that the adsorbed H<sup>+</sup> ions prevent the periodic movement (up-and-down and back-and-forth motions) of non-rigid zeolite-A framework only system.

The IR spectrum is calculated by Fourier transform of the total dipole moment auto-correlation function.<sup>19</sup> Figure 3 shows the calculated IR spectra of non-rigid dehydrated H<sub>12</sub>-A zeolite framework from our MD simulation. There are two major peaks, one around 2700 cm<sup>-1</sup> and the other around 7000 cm<sup>-1</sup>. The former appeared in the calculated IR spectra of non-rigid zeolite-A framework only system, indicating that the simple harmonic oscillation of the dipole moment autocorrelation function resulted in a very large sharp peak at 2700 cm<sup>-1</sup>, which reflects a monotonous dynamical feature of the framework.<sup>1</sup> But here the peak is very distorted probably due to the effect of the adsorbed H<sup>+</sup> ions. The latter also appeared in the calculated IR spectra of non-rigid zeolite-A framework only system, which was too small to be considered,<sup>1</sup> but here the corresponding peak is very large,

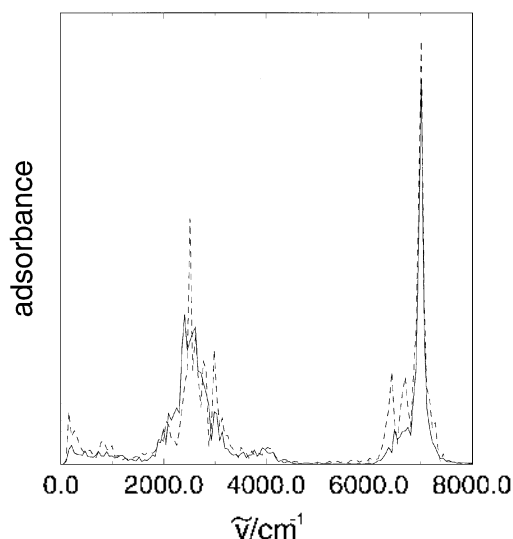


**Figure 3.** IR spectra of non-rigid dehydrated H<sub>12</sub>-A zeolite at 298.15 K, calculated from the total dipole moment autocorrelation function of zeolite-A framework. — :  $\sigma = 0.6$  and - - - - :  $\sigma = 1.4$   $\text{\AA}$ .

which remains unexplained except, perhaps, to indicating a new formation of a vibrational mode of the framework due to the adsorption of H<sup>+</sup> ions, which was not observed in non-rigid zeolite-A framework only system. For example, as discussed above, the MSD's of non-rigid dehydrated zeolite framework atoms (not shown) appear much different from those of non-rigid zeolite-A framework only system, which is all periodic.<sup>1</sup> This might be due to the adsorbed H<sup>+</sup> ions, which prevent the periodic movement of non-rigid zeolite-A framework only system. The different values of  $\sigma$  for H<sup>+</sup> ion affect the shape of the two peaks in the calculated IR spectra of non-rigid dehydrated H<sub>12</sub>-A zeolite framework. We also observed two nearly identical peaks in calculated IR spectra of non-rigid dehydrated Na<sub>12</sub>-A zeolite framework system.<sup>20</sup>

### Concluding Remarks

A molecular dynamics simulation of non-rigid dehydrated H<sub>12</sub>-A zeolite framework has been performed at 298.15 K, using the usual bond stretching, bond angle bending, torsional rotational, and non-bonded Lennard-Jones and electrostatic interactions for the intraframework interaction potentials. It is found that two different structures appear, depending on the choice of the Lennard-Jones parameter,  $\sigma$ , for the H<sup>+</sup> ion. For the smaller values of  $\sigma$  (0.6-1.2  $\text{\AA}$ ), the 12th H<sup>+</sup> ion is located on one of the 8-ring window sites that are already occupied by three H<sup>+</sup> ions. For the larger values of  $\sigma$  (1.3-1.8  $\text{\AA}$ ), it is at one of the opposite 4-ring sites with the remaining 11 H<sup>+</sup> ions almost kept near their initial positions. It is also found that some of the H<sup>+</sup> ions exchanged their sites without changing the number of H<sup>+</sup> ions at each site, which is often referred as "concerted transport process". The agreement between the experimental and calculated results for the zeolite-A framework atoms of structural parameters for non-rigid dehydrated zeolite A is generally quite good, but for the adsorbed cations the agreement is

somewhat poor. The calculated bond lengths are generally shorter than those obtained experimentally except for H<sub>1</sub>-O(3) due to the difference of Na<sup>+</sup> and H<sup>+</sup>. The calculated IR spectrum by Fourier transform of the total dipole moment auto-correlation function shows two major peaks, one around 2700 cm<sup>-1</sup> and the other around 7000 cm<sup>-1</sup>. The former appears in the calculated IR spectra of non-rigid zeolite-A framework only system and the latter remains unexplained, except, perhaps to indicating a new formation of a vibrational mode of the framework due to the adsorption of H<sup>+</sup> ions, which was not observed in non-rigid zeolite-A framework only system.

**Acknowledgment.** This work was supported by a research grant (KOSEF 951-0302-026-2) to SHL from the Korea Science and Engineering Foundation. The authors would like to thank the Computer Center at Korea Institute of Science and Technology for access to the Cray-C90 super computer and the Tongmyung University of Information Technology for access its IBM SP/2 computers.

### References

1. Lee, S. H.; Choi, S. G. *Bull. Kor. Chem. Soc.* **1998**, *19*, 422. In Table 2, T-O-T and O-T-O bond angle bending energies should be replaced by each other.
2. Moon, G. K.; Choi, S. G.; Kim, H. S.; Lee, S. H. *Bull. Kor. Chem. Soc.* **1992**, *13*, 317.
3. Moon, G. K.; Choi, S. G.; Kim, H. S.; Lee, S. H. *Bull. Kor. Chem. Soc.* **1993**, *14*, 356.
4. Lee, S. H.; Moon, G. K.; Choi, S. G.; Kim, H. S. *J. Phys. Chem.* **1994**, *98*, 1561.
5. Choi, S. G.; Lee, S. H. *Mol. Sim.* **1996**, *17*, 113. In Figs. 2, 3, 4, and 5, NII<sub>2</sub>(2) and NII<sub>3</sub>(3) should be replaced by each other.
6. Lee, S. H.; Choi, S. G. *J. Phys. Chem. B* **1997**, *101*, 8402.
7. Pluth, J. J.; Smith, J. V. *J. Am. Chem. Soc.* **1980**, *102*, 4704.
8. Nicholas, J. B.; Hopfinger, A. J.; Trouw, F. R.; Iton, L. X. *J. Am. Chem. Soc.* **1991**, *113*, 4792.
9. Faux, D. A.; Smith, W.; Forester, T. R. *J. Phys. Chem. B* **1997**, *101*, 1762.
10. Yanagida, R. Y.; Amaro, A. A.; Sell, K. *J. Phys. Chem.* **1973**, *77*, 805.
11. (a) de Leeuw, S. W.; Perram, J. W.; Smith, E. R. *Proc. R. Soc. London* **1980**, *A373*, 27. (b) Anastasiou, N.; Fincham, D. *Comput. Phys. Commun.* **1982**, *25*, 159.
12. Genechten, K. A. V.; Mortier, W. J. *Zeolites* **1988**, *8*, 273.
13. Chynoweth, S.; Klomp, U. C.; Scales, L. E. *Comput. Phys. Commun.* **1991**, *62*, 297.
14. Gauss, K. F. *J. Reine. Angew. Math.* **1829**, *II*, 232.
15. Gear, C. W. *Numerical initial value problems in ordinary differential equation*; Englewood Cliffs NJ, Prentice-Hall, 1971.
16. Shin, J. M.; No, K. T.; Jhon, M. S. *J. Phys. Chem.* **1998**, *92*, 4588.
17. Willis, B. T. M.; Pryor, A. W. *Thermal vibrations in Crystallography*; Cambridge University Press: Cambridge, 1975.
18. Johnson, C. K. ORTEP: A FORTRAN Thermal Ellipsoid Plot Program; ORNL-3794, Oak Ridge National Laboratory, Oak Ridge, TN, 9165.
19. Behrens, P. H.; Wilson, K. R. *J. Chem. Phys.* **1981**, *74*, 4872.
20. Lee, S. H.; Choi, S. G. submitted in *Bull. Kor. Chem. Soc.*